ARTICLE

BIOTECHNOLOGY and BIOENGINEERING

Three-Dimensional Cell Culture Microarray for High-Throughput Studies of Stem Cell Fate

Tiago G. Fernandes,[1,2] Seok-Joon Kwon,[1] Shyam Sundhar Bale,[1] Moo-Yeal Lee,[3] Maria Margarida Diogo,[2] Douglas S. Clark,[4] Joaquim M.S. Cabral,[2] Jonathan S. Dordick[1,5]

[1]Department of Chemical and Biological Engineering, Center for Biotechnology and Interdisciplinary Studies, Rensselaer Polytechnic Institute, Troy, New York; e-mail: dordick@rpi.edu

[2]Institute for Biotechnology and Bioengineering (IBB), Centre for Biological and Chemical Engineering, Instituto Superior Técnico, Lisboa, Portugal

[3]Solidus Biosciences, Troy, New York

[4]Department of Chemical Engineering, University of California, Berkeley, California

[5]Department of Biology, Rensselaer Polytechnic Institute, 110 8th Street, Troy, New York 12180; telephone: 518-355-4062; fax: 518-276-2207

This article was published online on 12 January 2010. An error was subsequently identified and the article was corrected on 24 February 2010

Received 26 September 2009; revision received 29 November 2009; accepted 23 December 2009

Published online 12 January 2010 in Wiley InterScience (www.interscience.wiley.com). DOI 10.1002/bit.22661

ABSTRACT: We have developed a novel three-dimensional (3D) cellular microarray platform to enable the rapid and efficient tracking of stem cell fate and quantification of specific stem cell markers. This platform consists of a miniaturized 3D cell culture array on a functionalized glass slide for spatially addressable high-throughput screening. A microarray spotter was used to deposit cells onto a modified glass surface to yield an array consisting of cells encapsulated in alginate gel spots with volumes as low as 60 nL. A method based on an immunofluorescence technique scaled down to function on a cellular microarray was also used to quantify specific cell marker protein levels in situ. Our results revealed that this platform is suitable for studying the expansion of mouse embryonic stem (ES) cells as they retain their pluripotent and undifferentiated state. We also examined neural commitment of mouse ES cells on the microarray and observed the generation of neuroectodermal precursor cells characterized by expression of the neural marker Sox-1, whose levels were also measured in situ using a GFP reporter system. In addition, the high-throughput capacity of the platform was tested using a dual-slide system that allowed rapid screening of the effects of tretinoin and fibroblast growth factor-4 (FGF-4) on the pluripotency of mouse ES cells. This high-throughput platform is a powerful new tool for investigating cellular mechanisms involved in stem cell expansion and differentiation and provides the basis for rapid identification of signals and conditions that can be used to direct cellular responses.

Biotechnol. Bioeng. 2010;106: 106–118.

KEYWORDS: stem cells; 3D cell culture; microarrays; high throughput; studies of stem cell fate

Introduction

Stem cells are characterized by their unlimited self-renewal capacity and potential to generate fully differentiated, mature cells (Smith, 2001). Due to these unique characteristics, stem cells are at the forefront of potential regenerative medicine therapies and may also provide an unlimited source of cells for pharmaceutical applications (Klimanskaya et al., 2008; McNeish, 2004). However, several major challenges hinder the development of new stem cell-based technologies. These challenges include the identification of new signals (e.g., small molecules, hormones, proteins, etc.) and conditions that regulate and influence cell function, and the application of this information toward the design of reproducible stem cell bioprocesses and therapies (Xu et al., 2008). Therefore, the ability to interrogate signals that influence stem cell fate in a high-throughput manner will greatly impact our understanding of the mechanisms that regulate cellular responses (Fernandes et al., 2009).

In this context, microscale technologies are emerging as powerful tools for tissue engineering (Khademhosseini

Correspondence to: J.S. Dordick

Contract grant sponsor: Fundação para a Ciência e a Tecnologia, Portugal
Contract grant number: BD/24365/2005
Contract grant sponsor: National Institutes of Health
Contract grant number: ES012619; GM66712

et al., 2006) and high-throughput screening (Lee et al., 2005, 2008), and as cell-based probes in chemical biology (Fernandes et al., 2008). With the advent of robotic spotting technology, it is now possible to distribute nanoliter volumes of different samples in a spatially addressable footprint (Anderson et al., 2005; Ko et al., 2005; Kwon et al., 2007). As a result, cellular microarrays can enable high-throughput, high-content (e.g., protein-specific) parallel screening of a large number of small molecules (Bailey et al., 2004). Such cell-based microarrays are particularly promising for studying the growth and differentiation of stem cells (Soen et al., 2006), and for investigating the influence of small molecules and cell growth conditions on cell physiology and function (Flaim et al., 2008).

The microarray format is therefore an attractive tool with a wide range of applications in cell biology and chemical biology that call for multiple experiments in parallel, while using minimal amounts of cells and often expensive reagents (Castel et al., 2006). While the complexity of signals required for stem cell expansion and lineage selection have prompted the development of microarray platforms for high-throughput screening of the effects of extracellular matrix proteins (Flaim et al., 2005), growth factors (Soen et al., 2006), and biomaterials (Anderson et al., 2004) on stem cell growth and differentiation, none of these systems used a three-dimensional (3D) environment. In addition to two-dimensional cell-culture arrays, miniaturized three-dimensional (3D) arrays have been developed, which are compatible with high-throughput screening (Lee et al., 2008). The more native-like microenvironment of the 3D culture may enhance the quality and biological relevance of the data that can be obtained in high-throughput screens (Horning et al., 2008; Hubbel, 2004). Despite these advances, 3D cellular microarrays for stem cell studies have not yet been fully developed.

In this article we present a high-throughput, 3D cell-based microarray platform designed to allow the expansion and differentiation of embryonic stem (ES) cells, while being compatible with high-throughput screening applications. As a model system, we have studied the expansion and neural commitment of mouse ES cells on arrays of microscale 3D alginate spots. Mouse ES cells were effectively expanded without differentiation in our platform, using serum-free media supplemented with leukemia inhibitory factor (LIF), or serum-free medium supplemented with LIF and bone morphogenetic protein-4 (BMP-4), demonstrating that a scale reduction of nearly 2,000-fold did not affect the performance of the culture. Under these conditions, cells retain their pluripotent state, which can be assessed by quantification of pluripotency markers such as Oct-4 or Nanog (Chambers et al., 2003; Niwa et al., 2000). However, under serum-free conditions, the absence of LIF leads to the neural commitment of mouse ES cells as a result of autocrine fibroblast growth factor (FGF) signaling (Ying et al., 2003b). By using a green fluorescent protein (GFP) knock-in reporter ES cell line it is possible to examine the process by which ES cells acquire neural identity in the cellular microarray, enabling the use of these platforms to promptly explore neural fate decisions in a 3D microenvironment. Moreover, as we demonstrate with FGF-4 and tretinoin, this system may also be tailored to examine in high-throughput fashion signals and conditions (e.g., small molecules and growth factors) that influence stem cell outcome. As a result, the identification of novel 3D microenvironments that regulate stem cell fate may be achieved using this platform.

Materials and Methods

Mouse ES Cell Culture Prior to Microarray Spotting

Upon thawing, 46C mouse ES cells (a kind gift from professor Austin Smith, University of Cambridge, UK) were expanded on gelatinized tissue culture plates at 37°C in a 5% CO_2 incubator (HEPA class100, Thermo, Waltham, MA), using serum-free ESGRO® complete medium (Millipore, Billerica, MA). The cells were trypsinized and seeded in each passage at 2×10^4 viable cells/cm^2, until further use for cell spotting on functionalized glass slides. After each passage, viable and dead cells were determined by counting in a hemocytometer using an optical microscope and the trypan blue dye (Invitrogen, Carlsbad, CA) exclusion test.

To evaluate the neural commitment of undifferentiated mouse ES cells following expansion, cells were trypsinized, plated on gelatin-coated tissue culture plates, and incubated for 6 days in RHB-A medium (Stem Cell Sciences, Edinburgh, Scotland, UK), as previously described (Diogo et al., 2008). At day 6, cells were recovered and analyzed by flow cytometry to quantify the population of Sox1-GFP$^+$ neural progenitor cells (Ying et al., 2003b).

Flow Cytometry

The percentage of Oct-4 and Nanog-expressing cells was evaluated by flow cytometry prior to microarray spotting. After expansion in tissue culture plates, cells were collected and fixed in 2% (w/v) paraformaldehyde (Sigma, St. Louis, MO) solution in PBS. Cells were then permeabilized with 1% (w/v) saponin (Sigma) solution in PBS, followed by incubation in blocking solution (3% (v/v) normal goat serum (NGS, from Sigma) in PBS) for 15 min. The primary antibody (mouse monoclonal anti-Oct-3/4 or rabbit polyclonal anti-Nanog (Santa Cruz Biotechnology, Santa Cruz, CA), 1:500 dilution in blocking solution) was added to the samples, and the cells were incubated for 2 h at room temperature. After washing thoroughly, the secondary antibody (Alexa Fluor® 488-conjugated goat-anti-mouse or goat-anti-rabbit IgG (Molecular Probes, Carlsbad, CA), 1:1,000 dilution in blocking solution) was added to the cells and the cells were incubated for 45 min at room temperature. After washing, the samples were analyzed by FACS. Cells incubated only with secondary antibody were used as negative control.

For the quantification of neural conversion, cells were trypsinized after neural commitment in tissue culture plates, resuspended in FACS buffer (PBS with 4% FBS), and analyzed by FACS. Settings were determined at the start of the experiment using undifferentiated 46C ES cells as negative control. Gates were set at 10 units of fluorescence, which excludes more than 99% of undifferentiated ES cells and dead cells.

All analyses were performed on a FACSCalibur™ flow cytometer (Becton Dickinson, Franklin Lakes, NJ) and CellQuest software. Cell debris and dead cells were excluded from the analysis based on electronic gates using forward scatter (size) and side scatter (cell complexity) criteria.

Glass Slide Modification

Borosilicate glass slides ($25 \times 75\,mm^2$, Fisher, Pittsburgh, PA) were pre-washed with ethanol and acid treated in concentrated sulfuric acid (98%) overnight, followed by sonication for 30 min, and washing in de-ionized distilled water and in acetone. The cleaned glass slides were dried using a nitrogen stream and then baked at 120°C for 15 min prior to use. To generate slides for cell spotting, the acid-cleaned glass slides were spin-coated at 3,000 rpm for 30 s with 0.1% (w/v) poly (styrene-*co*-maleic anhydride) (PS–MA, Sigma) in toluene solution as described previously (Lee et al., 2008). Methyltrimethoxysilane (MTMOS, Sigma)-coated slides were also prepared as described previously (Lee et al., 2005). These slides were used for small molecule printing and stamping experiments.

Mouse ES Cell Spotting and Expansion on Modified Glass Slides

A poly-L-lysine (PLL)–Ba^{2+} mixture was prepared by mixing a solution of $BaCl_2$ in water (0.1 M) and sterile PLL (0.01% (w/v)), both from Sigma, in a 1:2 volume ratio, respectively. This mixture was spotted on the PS–MA-coated glass slides using a MicroSys™ 5100-4SQ non-contact microarrayer (Genomic Solutions, Ann Arbor, MI). A mixture of low-viscosity alginate (Sigma) and cell suspension in growth medium was prepared and spotted on top of the $BaCl_2$/PLL bottom layer using the microarrayer. During cell spotting the humidity within the microarrayer chamber was maintained above 90% to retard water evaporation from the applied spots. The final concentration of alginate was 1% (w/v), while different cell densities were tested for these studies.

For mouse ES cell expansion, the slides were immersed in medium and incubated at 37°C in a 5% CO_2 incubator for 5 days. Two medium formulations were used: ESGRO® serum-free medium supplemented with 1% (v/v) penicillin (50 U/mL)/streptomycin (50 μg/mL) and 0.1% (v/v) fungizone® (both from Invitrogen); and Knockout® DMEM supplemented with 15% (v/v) Knockout® serum-replacement, 1% (v/v) L-glutamine 200 mM, 1% (v/v) penicillin (50 U/mL)/streptomycin (50 μg/mL), 0.1% (v/v) fungizone® (all from Invitrogen), 1% (v/v) non-essential amino acids 100× (Sigma), 0.1% (v/v) 2-mercaptoethanol 0.1 mM (Sigma), and 0.1% (v/v) LIF (10^6 U mouse LIF, Millipore). The medium was changed after 2 and 4 days in culture, and cellular viability was assessed with the LIVE/DEAD® Viability/Cytotoxicity Kit for mammalian cells (Invitrogen) (Lee et al., 2008). Briefly, the slides were rinsed three times in PBS and a solution containing 0.5 μM calcein AM was used to detect viable cells through green fluorescence intensity. The cell slides were gently dried and the fluorescence was immediately scanned (using the GenePix® Professional 4200A scanner, from Molecular Devices Co., Sunnyvale, CA) and quantified from the scanning image using the GenePix Pro 6.0 software package (Molecular Devices Co.). The blue laser (488 nm) for excitation and standard blue filter for green dye emission, and blue laser and 645AF75/594 filter for red dye were used for evaluating live and dead cells, respectively.

Neural Commitment of Mouse ES Cells on Cellular Microarray

A PLL–Ba^{2+} mixture was spotted on PS–MA-coated glass slides as described in the previous section. Prior to cell spotting, 46C mouse ES cells were expanded for two passages at 2×10^4 viable cells/cm^2, and then for one passage at a relatively high density (10^5 viable cells/cm^2) during 24 h in serum-free ESGRO® complete medium (Diogo et al., 2008). A mixture of low-viscosity alginate and cell suspension in culture medium was then prepared and spotted on top of the $BaCl_2$/PLL bottom layer using the microarrayer. Once again the humidity within the microarrayer chamber was maintained above 90% to retard water evaporation from the applied spots. The final concentration of alginate was 1% (w/v), while initial cell densities of 200 cells/spot or 400 cells/spot were tested for these studies. The slides were immersed in serum-free RHB-A medium supplemented with 1% (v/v) penicillin (50 U/mL)/streptomycin (50 μg/mL) and 0.1% (v/v) fungizone®, and incubated at 37°C in a 5% CO_2 incubator for 6 days. Medium was changed at days 2 and 4. The GFP fluorescence of Sox1-GFP^+ neural progenitors in the spots was visualized using a standard fluorescence microscope and quantified from the scanning image obtained using the slide scanner.

Cell-Based Microarray Immunofluorescence Assay: Oct-4 and Nanog Staining

Slides were rinsed in washing buffer (PBS containing 20 mM of $CaCl_2$), and cells were stained as described previously (Fernandes et al., 2008). Briefly, after fixing with a cold solution of methanol and acetone (1:1, v/v), slides were washed and incubated in blocking solution (SuperBlock™, Pierce, Rockford, IL). The primary antibody (mouse monoclonal anti-Oct-3/4 or rabbit polyclonal anti-Nanog, 1:500

dilution in PBS containing 0.1% (v/v) Tween-20 and 1% (w/v) BSA) was added to the slides and cells were incubated overnight at 4°C. After washing thoroughly, the secondary antibody (peroxidase-conjugated goat-anti-mouse or goat-anti-rabbit IgG, (Molecular Probes), 1:1,000 dilution in PBS containing 0.1% (v/v) Tween-20 and 1% (w/v) BSA) was added to the slides and cells were incubated for 3 h at room temperature. A tyramide signal amplification kit (Molecular Probes) was used following the manufacturer's instructions to detect the presence of the target protein through fluorescence analysis. The fluorescence levels of Oct-4 and Nanog were measured with a slide scanner and analyzed using GenePix Pro 6.0 (blue laser (488 nm) and standard blue filter for excitation/emission). The fluorescence signal of β-actin (determined using the same protocol using yellow laser (594 nm) and 645AF75/594 filter for excitation/emission) was used as the internal control.

Confocal Microscopy

Z-stacks were obtained using confocal microscopy to obtain 3D images of cell spots. Specifically, the cell nuclei of spotted cells were stained using DAPI (dilactate) (Invitrogen) by addition of 20 μL of 5 nM DAPI solution (λ_{ex}: 405 nm; λ_{em}: 460 nm) to cell slides in 10 mL of ESGRO® medium and incubated for 10 min. Stained samples were washed thoroughly with 10 mL of fresh medium at least three times before imaging. For obtaining the z-stack images, cell spots were imaged using a 10× objective with a section thickness of 4 μm.

Tretinoin and FGF-4 Incubation Using a Dual Slide Configuration

To demonstrate the potential of this platform for screening small molecules, growth factors, and their effects in stem cell models, 60 nL of known concentrations of tretinoin (all-*trans*-retinoic acid (RA) from Sigma) and FGF-4 (Sigma) were dispensed onto MTMOS-coated slides. The resulting array was then stamped on top of the 3D cellular array, in such a way that each compound-containing spot contacted a cell spot, as described previously (Fernandes et al., 2008; Lee et al., 2008). For efficient stamping, a 250-μm high silicone gasket was used to maintain proper spacing between the two slides (Lee et al., 2005), avoiding damage of the alginate spots while maintaining an optimal distance between the cell spots and the compound-containing spots during incubation. The dual slide system was subsequently incubated for specific times at 37°C in a humidified hybridization chamber to prevent evaporation and spot drying. After stamping, the cell spots were rinsed with warm medium and the cellular microarray was incubated at 37°C in serum-free ESGRO® complete medium for 3 days, and finally stained for Oct-4 and Nanog using the cellular microarray-based immunofluorescence assay described previously.

Statistical Analysis

Statistical analysis was performed using the SPSS 16.0 software (SPSS, Inc., Chicago, IL, http://www.spss.com.uk). The non-parametric Wilcoxon–Mann–Whitney test was used to evaluate statistical significance of two independent samples ($P < 0.05$). Error bars represent the standard error of the mean (SEM) from triplicate slides for each condition (total of 144 spots for each point).

RESULTS

Cellular Microarray Fabrication and Characterization

Signals provided by the stem cell microenvironment, or niche, are essential for controlling stem cell fate. These signals include physical cues, such as matrix elasticity (Engler et al., 2006), cell–cell and cell–ECM interactions, soluble factors (e.g., growth factors and small molecules), and the 3D architecture that supports cell growth and differentiation (Even-Ram et al., 2006). In an effort to mimic this intricate niche, we used a 3D cell-on-a-chip technique involving alginate-based matrixes on a microscope slide that was recently developed by Lee et al. (2008). The glass surface of the slide was treated and functionalized using a reactive copolymer of polystyrene and maleic anhydride (PS–MA; Fig. 1A) in order to increase surface hydrophobicity while providing reactive groups to covalently attach the highly cationic PLL. A bottom layer of PLL and $BaCl_2$ was spotted onto predetermined positions of the PS–MA-treated surface. 3D spots were formed by the deposition of an alginate solution containing cells on top of the PLL/$BaCl_2$ bottom layer. Under these conditions, the positively charged PLL serves as a substrate to bind Ba^{2+} ions and assist the attachment of the negatively charged alginate. The Ba^{2+} ions cause instantaneous gelation of alginate chains to give rise to 3D cell-containing matrix spots (60 nL) with a diameter of <800 μm and a center-to-center distance between adjacent spots of <1,200 μm (Fig. 1B). This spotting technique is reproducible and requires low amounts of reagents for fabrication of the biochip, producing a functional microarray platform for high-throughput screening compatible with conventional microarray scanning for quantitative studies.

The capacity of the microscale 3D alginate matrix to support mouse ES cell growth was also evaluated. Arrays of 560 spots with 46C mouse ES cells at an initial cell density of 100 cells/spot were prepared and incubated in serum-free expansion medium (ESGRO® complete) for 5 days. During this period, the cells remained confined within the spots, with no spot breakage and no visible gel detachment from the slide, indicating that the spots were structurally stable. Confocal microscopy images (of 30 nL spots) also indicate that encapsulated cells are evenly distributed inside the alginate spots and are in fact organized in a 3D environment (Fig. 1C). Cell viability was confirmed after 5 days by

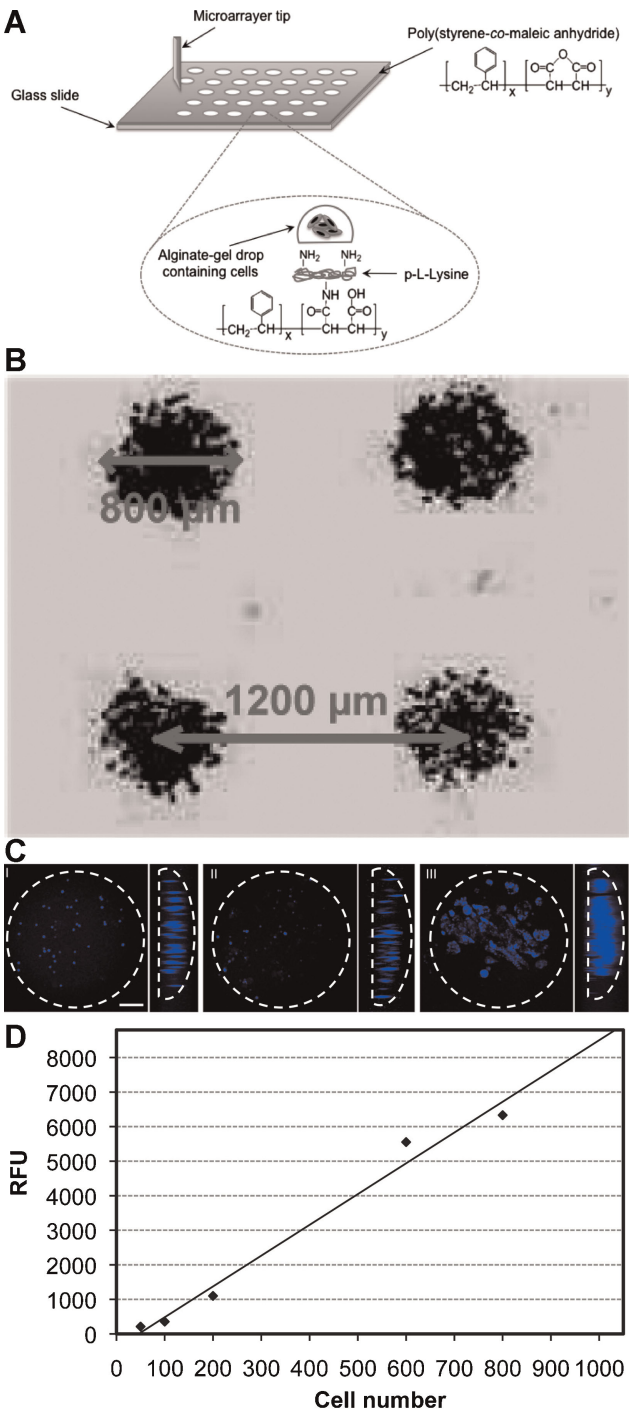

Figure 1. 3D cellular microarray platform for mouse ES cell culture. **A**: Cell encapsulation on a functionalized glass slide. The cells are spotted on PS–MA modified glass slides using a microarray spotter. **B**: Light microscope image of a portion of the cellular microarray (60 nL spots) depicting the spot diameter and center-to-center distance between adjacent spots. **C**: Confocal microscopy images showing the three-dimensional distribution of mouse ES cells on day 0 (I), day 2 (II), and day 5 (III) of incubation. Shown in each panel is the top view and side view of the spot, from a z-stack obtained with 4 μm sections. Scale bar is 100 μm. Each spot is 30 nL resulting in a diameter of 560 μm and a height of 150 μm. **D**: Correlation of fluorescence intensity (RFU) of calcein AM staining integrated over the spot area with the number of viable cells present in the spot. [Color figure can be seen in the online version of this article, available at www.interscience.wiley.com.]

staining a slide with the fluorescent dyes calcein AM and ethidium homodimer-I to identify live and dead cells, respectively (data not shown). Red fluorescence of dead cells was negligible when compared to green fluorescence of live cells, indicating that the hydrogel environment did not seriously affect cell viability, a result in agreement with previous studies of ES cell encapsulation in alginate hydrogels (Siti-Ismail et al., 2008). Moreover, live cell numbers per spot correlated linearly with green fluorescence intensity (Fig. 1D), which facilitated cell growth calculations (Fernandes et al., 2008; Lee et al., 2008).

Mouse ES Cell Expansion in 3D Alginate-Matrix Spots

To assess the suitability of the microscale 3D alginate matrix for mouse ES cell culture, arrays of 560 spots containing 46C cells were created at different initial densities per spot (Table I). Increased seeding cell densities resulted in lower growth rates of the cells, as reflected by the observed doubling times. Mixtures of low-viscosity alginate and cell suspension in expansion medium were prepared and spotted on top of the $BaCl_2$/PLL bottom layer using a robotic spotter. After spotting, the slides were maintained in expansion medium for 5 days, followed by staining of viable cells in the spot microenvironment using a calcein AM fluorescent dye (Fig. 2A). Two serum-free expansion media were tested: ESGRO® complete medium, and DMEM supplemented with Knockout® serum-replacement (DMEM/SR) and LIF. Under serum-free conditions, both expansion media support mouse ES cell expansion, either by the combination of LIF and serum-replacement, or by the combination of LIF and BMP-4 (in the case of ESGRO® complete), which act together to sustain self-renewal capacity and preserve multilineage differentiation potential of mouse ES cells (Ying et al., 2003a).

The evolution of viable cell number on alginate gel spots throughout time in culture can be seen in the growth curves presented in Figure 2B. Cells were inoculated at 50, 100, 200, and 400 cells/spot on 60 nL spots in ESGRO® complete medium or DMEM/SR medium supplemented with LIF. Cell growth could be observed at all initial cell densities tested. For lower initial cell densities (50 and 100 cells/spot), similar results were obtained for both expansion media. Cells expanded exponentially for the first 2 days in culture and then more slowly until day 5, reaching an average number of viable cells per spot close to 1,000. At higher seeding densities (200 and 400 cells/spot), expansion in ESGRO® complete medium led to an exponential phase of cell growth until day 3, after which the maximum fold increase in total cells was obtained, followed by a stationary phase until day 5 in culture. On the other hand, when DMEM/SR supplemented with LIF was used for the expansion of cells seeded at 200 or 400 cells/spot, cell growth was slower and a stationary phase was only reached at day 4. However, the final cell number per spot obtained for both growth media was comparable by day 5 (~1,300 cells/spot

Table I. Cell seeding density, number of cells per spot, and doubling times for mouse ES cell expansion on 3D cellular microarrays.

Seeding density (cells/mL)	Spot volume (nL)	Cells/spot	Doubling time (h)	
			ESGRO®	DMEM/SR + LIF
8.3×10^5	60	50	17.0 ± 0.4	22.6 ± 0.3
1.7×10^6	60	100	18.4 ± 0.4	21.3 ± 0.3
3.3×10^6	60	200	26.3 ± 0.5	30.8 ± 0.3
6.7×10^6	60	400	30.4 ± 0.2	39.8 ± 0.4

ESGRO®: cells expanded for 5 days in ESGRO® complete serum-free medium; DMEM/SR + LIF: cells expanded for 5 days in Knockout® DMEM supplemented with 15% Knockout® serum replacement and LIF; doubling time values represent mean ± SEM.

and ~1,700 cells/spot for initial seeding densities of 200 and 400 cells/spot, respectively).

Cell expansion in terms of fold increase in total cell number was similar for both growth media tested in all seeding densities under study. However, this value decreased by increasing initial cell density (Fig. 2C). This may be related to cell growth inhibition due to higher accumulation of toxic metabolic waste products in the spot microenvironment, and also less space available for cell growth inside the alginate matrix. A similar trend could be seen for the apparent specific growth rate calculated for each seeding density (Fig. 2C), and the corresponding doubling time (Table I). The higher specific growth rate (μ_{max}) was obtained for an initial cell density of 50 cells/spot in ESGRO® complete medium (1.0 ± 0.03 day^{-1}, with a doubling time (t_d) of 17.0 ± 0.4 h); these values are comparable to those obtained for 46C mouse ES cell expansion in well plate cultures or spinner flasks ($\mu_{max} = 1.0 \pm 0.2$ day^{-1} and $t_d = 16.6 \pm 3.3$ h) (Fernandes et al., 2007, 2010). 46C mouse ES cells could thus be cultured in the microarray platform without losing viability, and the culture performance was not affected by the near 2,000-fold scale reduction from typical tissue culture plate systems.

Mouse ES Cells Retain Their Undifferentiated State in the Cellular Microarray

Typically, ES cells express several markers of pluripotency such as Oct-4 and Nanog, among others (Chambers et al., 2003; Niwa et al., 2000). Thus, when expanded in the presence of LIF, mouse ES cells express high levels of Oct-4 and Nanog, as was confirmed by flow cytometry after intracellular staining (Fig. 3A). In order to quantify the levels of these proteins in situ, we used an in-cell, on-chip immunofluorescent methodology to enable rapid quantification of the levels of specific cell marker proteins on the microarray platform (Fernandes et al., 2008).

Briefly, after fixing and permeabilizing the cells, a primary antibody specific to the target protein was added to the chip. A strong signal was obtained by using a horseradish peroxidase (HRP) secondary antibody complex that binds to the primary antibody. The HRP generates multiple copies of a tyramide dye that is highly reactive and covalently attaches to nucleophilic residues in the vicinity of the HRP–target interaction site, minimizing diffusion-related loss of signal and enabling quantification of the target protein in each individual spot without spot-to-spot contamination (Fernandes et al., 2008). In the present work, this procedure was used to stain mouse ES cells encapsulated in the alginate spots after expansion for 5 days in serum-free medium containing LIF. As expected, cells stained positively for Oct-4 (Fig. 3B), demonstrating that expansion in the 3D alginate matrix did not result in loss of Oct-4 expression.

The in-cell, on-chip immunofluorescence method also enables quantitative analysis of both Oct-4 and Nanog markers, thereby providing an opportunity to perform cell fate studies in a high-throughput fashion. To test this possibility, we expanded mouse ES cells in the alginate spots for 5 days in serum-free medium either in the presence or in the absence of exogenous LIF. Histogram plots showing the distribution of Oct-4 and Nanog (normalized for β-actin) signals for these two conditions obtained from separate slides can be seen in Figure 3C. The analysis of the distribution of both signals reveals two distinct cell populations. The absence of LIF supplementation essentially causes spontaneous differentiation of cells within the alginate spots, with concomitant decrease in both markers of pluripotency. Although Oct-4 and Nanog expression is not completely lost, their levels significantly decreased in comparison to expansion in the presence of LIF ($P < 0.05$) (Fig. 3D). This observation was independent of the initial cell density tested (50 or 100 cells/spot). However, a greater difference was evident for an initial cell density of 50 cells/spot, especially in the case of Oct-4. Under these conditions, in the absence of LIF, the Oct-4 signal was only $34 \pm 3\%$ of that measured for cells expanded in the presence of exogenous LIF. For an initial cell density of 100 cells/spot, this difference was $51 \pm 2\%$. This result shows a greater susceptibility for spontaneous differentiation in cells seeded at lower densities in the alginate spots and maintained without LIF. This may be related to a supportive role of endogenous STAT-3 signaling in maintaining cell pluripotency in the absence of exogenous LIF (Davey and Zandstra, 2006). Although insufficient for sustaining self-renewal, endogenous STAT-3 signaling can delay, at least to some extent, spontaneous differentiation. However, this process is more efficient when cells are in close proximity, which is

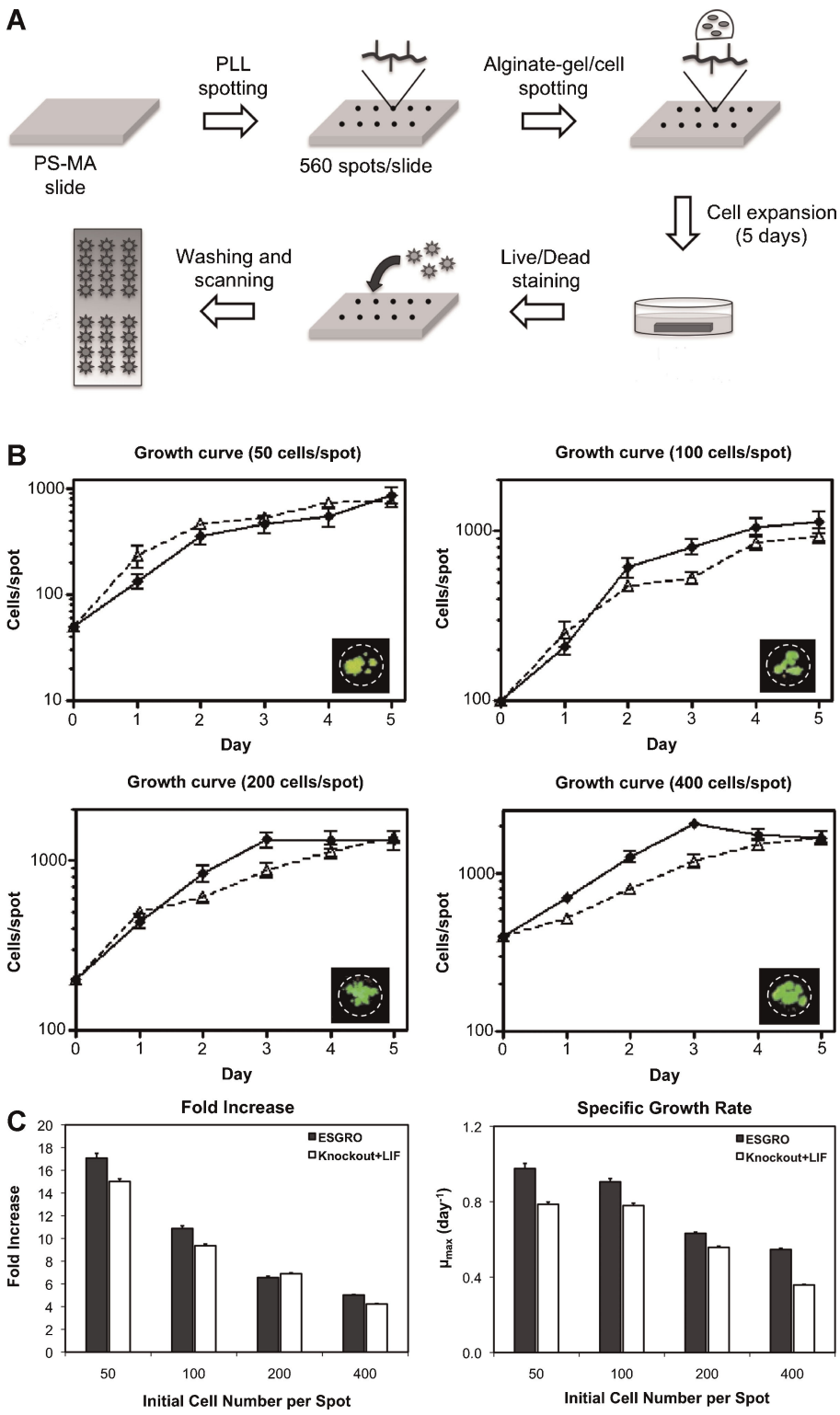

Figure 2. Mouse ES cell expansion in the 3D cellular microarray platform. **A**: Schematic representation of cell encapsulation on functionalized glass slides, followed by expansion in serum-free medium, and staining of viable cells in the spot microenvironment. **B**: Growth curves in terms of viable cell number of 46C mouse ES cells expanded in alginate gel spots. Cells were inoculated at 50, 100, 200, and 400 cells/spot on 60 nL spots in ESGRO® complete medium (black diamonds) and DMEM/SR medium supplemented with LIF (white triangles). Insets show a fluorescence-scanning image of representative alginate spots (800 μm in diameter) after expansion for 5 days at each seeding density used. Calcein AM was used to detect viable cells through green fluorescence. **C**: Comparison between the four initial cell densities tested. Cell expansion in terms of fold increase in total cell number and maximum specific growth rates were calculated for cells inoculated at 50, 100, 200, and 400 cells/spot on 60 nL spots in ESGRO® complete medium (black bars) and DMEM/SR medium supplemented with LIF (white bars). All error bars show the standard error of the mean ($n = 3$ slides, 144 spots in total for each data point). [Color figure can be seen in the online version of this article, available at www.interscience.wiley.com.]

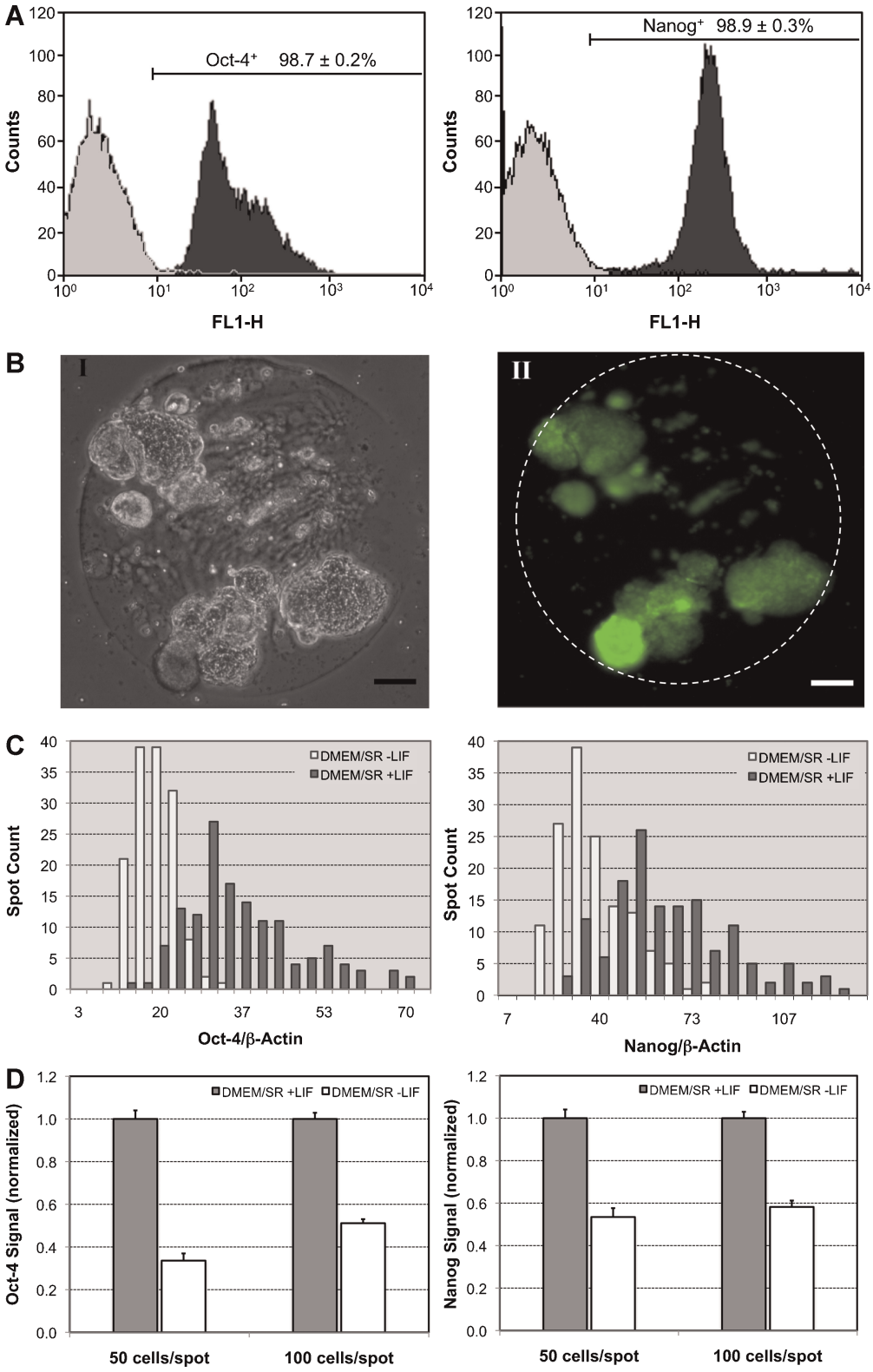

Figure 3. Mouse ES cells retain their undifferentiated state after expansion in the alginate spots. **A**: Mouse ES cells express high levels of Oct-4 and Nanog prior to spotting in the microarray, as can be seen by flow cytometry. **B**: Following expansion for 5 days in the alginate spots in serum-free medium containing LIF, mouse ES cells stain positively for Oct-4. Cells were inoculated at 100 cells/spot on 60 nL spots in DMEM/SR medium supplemented with LIF (**I**: bright field; **II**: fluorescence; scale bar: 100 μm). **C**: Histogram plots showing the distribution of Oct-4 and Nanog (normalized for β-actin) signals for cells expanded during 5 days in serum-free medium in the presence of LIF (+LIF) or absence of LIF (−LIF). **D**: Quantification of Oct-4 and Nanog using the in-cell, on-chip immunostaining method. Cells were inoculated at 50 or 100 cells/spot on 60 nL spots and were expanded in serum-free medium in the presence of LIF (+LIF) or absence of LIF (−LIF). Oct-4 and Nanog signals were normalized for β-actin and are relative to +LIF conditions. [Color figure can be seen in the online version of this article, available at www.interscience.wiley.com.]

more likely to happen when cells are seeded at higher initial cell densities.

Overall, the on-chip immunofluorescence method proved to be adequate for measuring levels of Oct-4 and Nanog in response to LIF stimulation. Moreover, mouse ES cells retained their undifferentiated state after expansion in the 3D alginate spots when LIF was exogenously supplemented to the culture medium.

Neural Commitment of Mouse ES Cells in 3D Alginate Spots

The utility of ES cells as a source of defined cell populations for pharmaceutical screening or clinical transplantation is largely unfulfilled because in vitro differentiation is still poorly controlled. However, mouse ES cells commit efficiently to a neural fate in adherent monoculture when signals for alternative fates are eliminated (Ying et al., 2003b). This process requires autocrine FGF signaling, and we reasoned that the alginate matrix could provide an optimal microenvironment for this process to take place.

A Sox1-GFP knock-in mouse ES cell line (46C) was used to investigate the neural commitment in a microscale cell chip environment. Sox1 is the earliest known specific marker of the neuroectoderm in the mouse embryo, and in serum-free conditions withdrawal of LIF results in the emergence of Sox1-GFP$^+$ cell phenotype in a rosette conformation typical of neuroepithelial cells (Ying et al., 2003b). Using flow cytometry quantification, it is possible to determine that a high percentage of ES cells (>80%) is able to undergo neural conversion (Fig. 4A). To evaluate the neural commitment of 46C mouse ES cells in situ, cells were spotted onto the 3D cell culture microarray and were cultured for 6 days in RHB-A medium. The cells were able to grow in these conditions, and after 6 days they organized into tubular-like structures and rosette conformations typical of early neural progenitors (Ying et al., 2003b) (Fig. 4B-I). Furthermore, they were Sox1$^+$, which was confirmed by the green fluorescence resulting from GFP expression (Fig. 4B-II). A histogram plot showing the distribution of Sox1-GFP (normalized for β-actin) signal for cells that underwent neural commitment and pluripotent cells revealed that it is possible to distinguish these two cell populations in the microarray platform based on Sox1 expression (Fig. 4C). Quantification of GFP signal and markers of pluripotency (Oct-4 and Nanog, measured using the on-chip immunofluorescent method) in cells cultured under neural commitment conditions (RHB-A), and cells cultured under expansion conditions (DMEM/SR + LIF), further indicates significant differences in terms of cell fate. Sox1$^+$ cells show negligible expression of Oct-4 and Nanog when compared with pluripotent cells (Fig. 4D). On the other hand, pluripotent cells do not express Sox1 (Ying et al., 2003b) and the GFP signal measured across the microarray spots was significantly lower ($P < 0.05$) than that measured for cells committed with the neural lineage. However, in the case

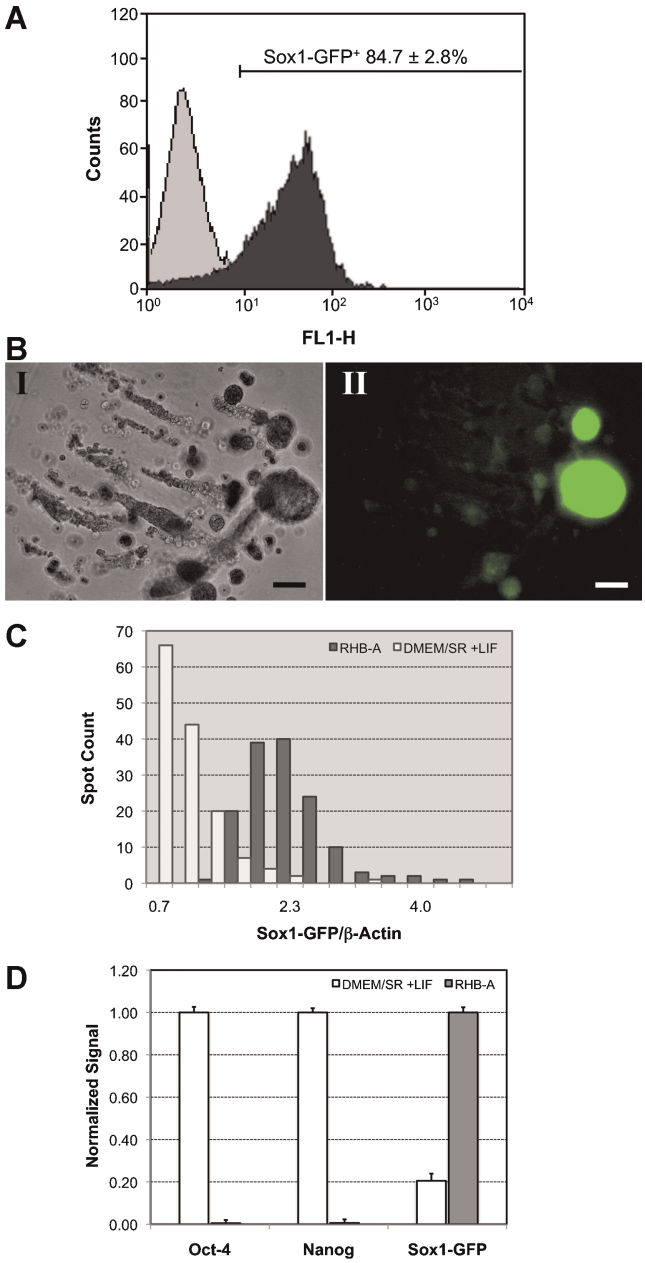

Figure 4. Neural commitment of mouse ES cells on the cellular microarray. **A**: Neural committed cells express high levels of Sox1, a marker of primitive neuroectoderm, as can be seen by flow cytometry after culture on tissue culture plates. **B**: After incubation for 6 days in the alginate spots in RHB-A serum-free medium, mouse ES cells differentiate into Sox1-GFP$^+$ neural precursor cells. The image shows a magnification of the center of a cell-containing alginate spot. Cells were inoculated at 400 cells/spot on 60 nL spots (**I**: bright field; **II**: fluorescence; scale bar: 100 μm). **C**: Histogram plot showing the distribution of Sox1-GFP (normalized for β-actin) signal for cells cultured for 6 days in RHB-A serum-free medium. **D**: Quantification of Oct-4, Nanog, and Sox1-GFP for cells expanded in serum-free medium in the presence of LIF (DMEM/SR + LIF) and cells cultured for 6 days in RHB-A serum-free medium. Oct-4 and Nanog signals were normalized for β-actin and are relative to cells expanded in DMEM/SR + LIF. Sox1-GFP signals were normalized for β-actin and are relative to cells cultured in RHB-A medium. [Color figure can be seen in the online version of this article, available at www.interscience.wiley.com.]

of Sox1-GFP, the fluorescent signal is directly measured from the microarray without signal amplification using an immunostaining method, which results in a residual signal in pluripotent cells (Sox-1$^-$) due to intrinsic fluorescence of the cells.

These results show that the microarray system provides a suitable platform for studying the molecular mechanisms of neural commitment and potentially to optimize the efficiency of neuronal cell production from pluripotent mammalian stem cells in a high-throughput manner. In a broader context, a similar approach could be adopted to study different cellular processes and gain a deeper understanding of stem cell differentiation.

Tretinoin and FGF-4 Incubation Using a Dual Slide Configuration

The high-throughput capacity of our microarray platform was also tested by spotting tretinoin (all-*trans*-RA) and FGF-4 in arrays of 60-nL spots printed onto MTMOS-coated slides. This approach was used to demonstrate the potential of this platform for screening small molecules, and combination of small molecules with growth factors, and their effects on stem cell models. To facilitate the addition of these compounds onto the cell-containing microarray, an MTMOS-coated glass slide was prepared and spotted with specific concentrations of RA and FGF-4. The MTMOS slide is complementary to the 3D cell-containing alginate array. Bringing both slides together via stamping, followed by incubation, provides a dual slide system that enables the small molecules to diffuse into the cell spots and induce a biological response (Fig. 5A). The diffusion of small molecules through alginate spots is expected to be fast due to the high water content of the gel (Ha et al., 2008). In fact, the widespread use of alginate cell-based encapsulation is due to the gentle environment alginate provides to the entrapped cells, as well as its high porosity due to the open lattice structure in the gel. This allows for high molecular (small

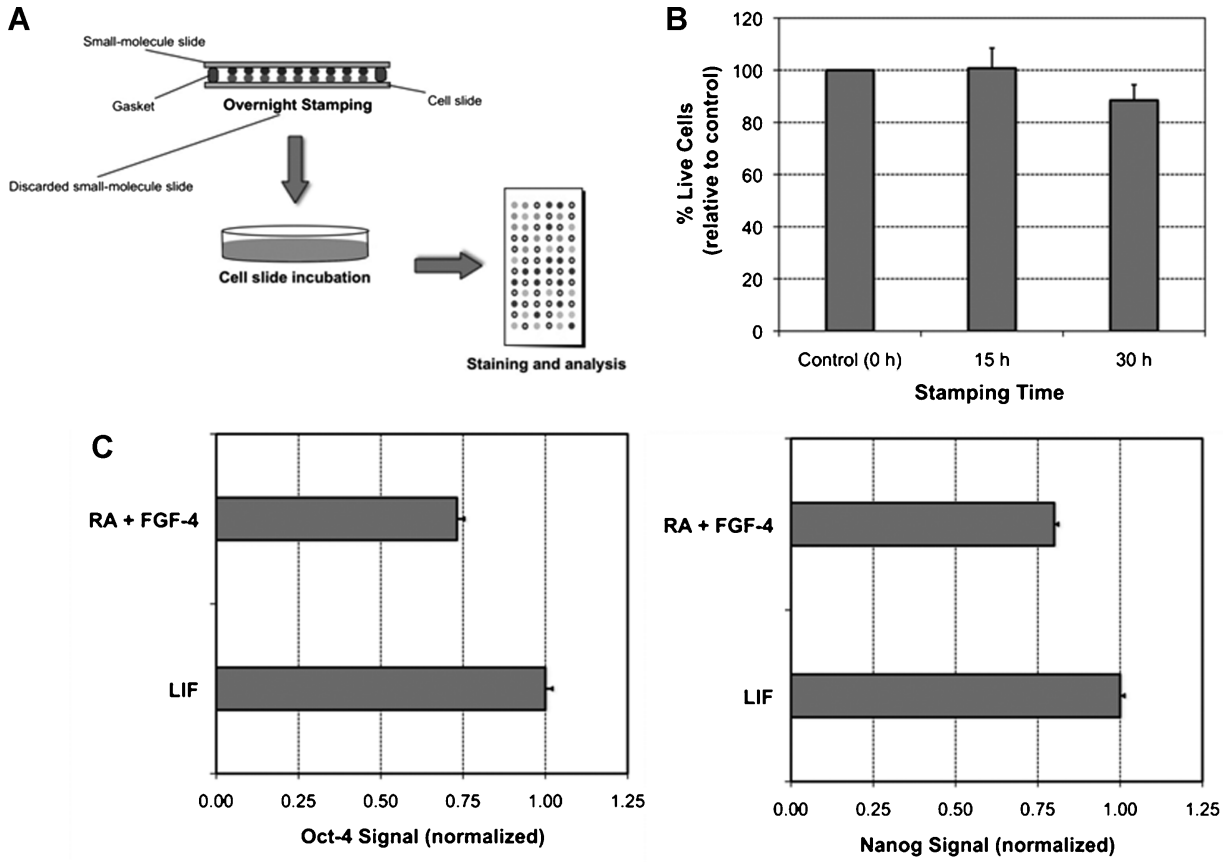

Figure 5. Cellular microarray platform is compatible with high-throughput studies. **A**: Schematics depicting the dual slide incubation procedure. FGF-4 (2 ng/mL) and retinoic acid (10 μM) were printed onto MTMOS-functionalized glass slides and stamped on top of alginate spots containing mouse ES cells. LIF was used as positive control. The dual slide system was incubated overnight and cells were incubated for additional 3 days before analysis. **B**: Percentage of viable cells after stamping using a dual slide system and incubation for specific times at 37°C in a humidified chamber. After stamping, the cellular microarray was incubated in expansion medium (ESGRO® complete) for 3 days, and finally stained using the calcein AM viability dye. The results are normalized for the levels of the control (no stamping) cells. **C**: Quantification of Oct-4 and Nanog levels on the 3D cellular microarray after stamping with FGF-4 (2 ng/mL) and retinoic acid (10 μM), or LIF, and subsequent incubation in LIF-containing medium for 3 days. The results are normalized for the levels obtained with LIF. β-Actin was used as the internal control.

molecule and protein growth factor) rates of diffusion within the whole gel structure and facilitates exchange with aqueous solutions (Oyaas et al., 1995). Thus, for the stamping time used in this work, the molecules would diffuse a distance much greater than the height of the stamped spots (~150 μm). A similar stamping strategy was already shown to be effective in the high-throughput analysis of small molecule cytotoxicity in human hepatoma and breast cancer cell lines (Lee et al., 2008).

MTMOS-coated slides were printed with RA (10 μM) and FGF-4 (2 ng/mL) in a block of 14 × 20 spots. The printed MTMOS slides were stamped afterwards on top of the 3D cell-containing alginate array (also prepared in a spot arrangement that was a mirror image of the small-molecule-containing slide), such that each small-molecule spot was in contact with a cell spot, as previously described. The stamped slides were incubated overnight, after which the slides were separated and cells were incubated for additional 3 days before analysis (Fig. 5A). A block of 14 × 20 spots printed in the same slide with expansion medium supplemented with LIF was used as a control. The stamping did not affect the cell viability, which remained high and comparable to cells that were not subjected to this process (Fig. 5B). This is due to the fact that incubation of the dual slide system was performed in a humidified chamber to prevent spot drying and consequent cell death.

It was expected that overnight stamping with a mixture of RA and FGF-4, despite being a relatively short time, would result in irreversible differentiation of cells and consequently a decrease in the expression of pluripotency markers, since both molecules are involved in signaling pathways that lead to mouse ES cell differentiation (Kim et al., 2009; Ying et al., 2008). Quantification of Oct-4 and Nanog levels on the 3D cellular microarray after stamping and subsequent incubation in LIF-containing medium for 3 days revealed that cells subjected to a combination of RA and FGF-4 in fact decreased levels of these markers (Fig. 5C). Although not particularly pronounced (approximately a 25% decrease for Oct-4 and 20% for Nanog, respectively), this reduction was statistically significant ($P < 0.05$) when compared to the levels registered when LIF was stamped instead. This result supports our initial assumption that despite the relatively short stamping time with the molecules, the combination of RA and FGF-4 induced cell differentiation, wherein cells could not recover Oct-4 and Nanog levels of expression even after incubation in LIF-containing medium for an additional 3 days. This provides proof of concept of the use of our system to examine, in high-throughput, signals and conditions that influence stem cells. Therefore, the identification of novel in vitro 3D microenvironments that regulate stem cell fate may be achieved using this platform.

Discussion

Stem cells are known to reside in complex microenvironments, or niches, that regulate their self-renewal and differentiation (Morrison and Spradling, 2008). Signals emanating from the stem cell niche include physical cues and soluble factors arranged in a 3D topography of controlled stiffness. Mimicking this intricate niche is expected to facilitate the ex vivo control of stem cell self-renewal and differentiation (Dellatore et al., 2008).

Herein we proposed a novel cellular microarray platform that includes some of the features described above for the stem cell niche, namely its three-dimensionality (Fig. 1). In general, cellular microarrays are powerful tools that enable the multiplexed interrogation of living cells and the analysis of cellular responses in a high-throughput manner (Fernandes et al., 2009). However, it has been shown that the 3D architecture of the cellular niche improves the quality of data obtained from in vitro assays (Horning et al., 2008). Therefore, in an effort to create a 3D cell-chip platform, we used a technique involving an alginate-based matrix on a microscope slide. Alginate is a biocompatible hydrogel and its use results in stable 3D spots that support cell growth (Fig. 1B and C). The reticulate structures formed by crosslinked alginate chains possess high water contents that facilitate the transport of nutrients, soluble factors, and waste products in the spots, while effectively encapsulating the cells inside. Therefore, this approach produces a functional microarray platform for high-throughput screening compatible with 3D stem cell growth.

The functionality of the system was first tested by creating arrays of cells at different initial cell densities per spot, and evaluating the expansion of these cells in the presence of LIF (Fig. 2 and Table I). We analyzed cell expansion in these conditions and calculated the apparent specific growth rate for each seeding density and the corresponding doubling time. As shown previously for 2D culture in patterned substrates (Dike et al., 1999), different initial cell densities may result in different cellular outcomes. In this work, we also observed an influence of the initial cell density in the expansion of mouse ES cells on alginate-matrix spots; namely, that higher seeding densities led to lower fold increases in total cell number and lower specific growth rates. This may be related with cell growth inhibition due to lack of space available for cell growth inside the alginate matrix, and also to higher accumulation of toxic metabolic waste products in the spot microenvironment when cells are seeded at higher numbers. Interestingly, in the presence of LIF, these cells express high levels of pluripotency markers; thus, the reduction in the apparent specific growth rate is not related to differentiation in the spots. More important, the culture performance was not affected by the near 2,000-fold scale reduction from typical well plates cultures, since growth rate values were comparable to those obtained for mouse ES cell expansion in larger scale culture systems.

The ability to quantify the levels of specific cell marker proteins and track cell fate decisions on the microarray platform was also tested. To this end, we used an immunofluorescence method that was scaled down to function at the microscale level and allow high-throughput analysis of target proteins (Fernandes et al., 2008). We

evaluated the levels of the pluripotency markers Oct-4 and Nanog in situ, and the in-cell, on-chip immunofluorescence methodology was found to be both sensitive and accurate for measuring levels of these proteins in response to LIF stimulation (Fig. 3). Specifically, when LIF was added to the growth medium, cells expanded in the alginate spots stained positively for both Oct-4 and Nanog. Furthermore, the cells showed high levels of expression of these markers, especially when compared to cells expanded in the absence of exogenous LIF. In this case, although a serum-free medium was used, the presence of signals in the serum-replacement supplement caused spontaneous differentiation, which resulted in significant decrease in the expression of pluripotency markers. Hence, mouse ES cells retained their undifferentiated state after expansion in the 3D alginate spots when LIF was exogenously supplemented to the culture medium. However, when signals for alternative fates are eliminated, ES cells commit efficiently to a neural fate as a consequence of autocrine FGF signaling (Ying et al., 2003b). Such a cell fate could also be evaluated using our microarray platform (Fig. 4). The use of a Sox1-GFP knock-in mouse ES cell line allowed us to quantify the levels of Sox1 expression that resulted of the neural commitment of cells. The alginate-matrix provided a favorable microenvironment for this process to take place, and after 6 days of neural commitment cells showed high levels of Sox1 expression and negligible levels of both Oct-4 and Nanog (Fig. 4D). Overall, this system provides a suitable platform for studying the molecular mechanisms of neural commitment in a high-throughput manner and may also be tailored to study different processes and gain a deeper understanding of stem cell differentiation.

Finally, the high-throughput capacity of our microarray platform was tested using a dual slide system where MTMOS-coated slides spotted with a mixture of RA and FGF-4 were stamped on top of a 3D cell-containing alginate array that was a mirror image of the small-molecule-containing slide (Fig. 5). We used this approach to demonstrate the potential of this platform for screening small molecules and their effects in stem cell models. Bringing both slides together via stamping, followed by incubation, provides a dual slide system that enables the small molecules to diffuse into the cell spots and induce a biological response (Lee et al., 2008). Overnight stamping with a mixture of RA and FGF-4 was expected to result in irreversible differentiation of cells and consequent decrease in the expression of pluripotency markers even after incubation in LIF-containing medium for additional 3 days. Quantification of Oct-4 and Nanog levels on the 3D cellular microarray after stamping and subsequent incubation in LIF-containing medium supported this assumption (Fig. 5C), showing that despite the relatively short stamping time with the molecules, the combination of RA and FGF-4 induced cell differentiation and cells could not recover Oct-4 and Nanog levels of expression. This procedure illustrates that the 3D cellular microarray can be tailored to function as a high-throughput screening platform to evaluate simultaneously the effects of different molecules, either alone or in combination, on stem cell fate.

Conclusions

Due to their unique characteristics, stem cells find potential applications in the areas of regenerative medicine and drug discovery. Therefore, it is crucial to expedite our knowledge on the fundamental aspects of stem cell self-renewal and differentiation. We have developed a microarray-based platform that can be used to study these events with minimal consumption of cells and reagents. Furthermore, cells can be expanded and differentiated in a 3D alginate-matrix environment in a highly parallel fashion. In conclusion, the 3D cellular microarray presented herein serves as a high-throughput platform that enables quantification of on-chip cellular protein levels following perturbation of stem cells upon addition of soluble factors. This method should have many applications in high-content, cell-based screening regimens for the discovery of new agents and conditions that control stem cell fate. In a broader context, this cellular microarray may be further expanded to other applications such as high-throughput drug screening, enzyme inhibition, and cytotoxicity assays.

T.G.F. acknowledges support from Fundação para a Ciência e a Tecnologia, Portugal (BD/24365/2005). J.S.D. and D.S.C. acknowledge support from the National Institutes of Health (ES012619 and GM66712).

Note Added in Proof

Corrections were made after initial online publication to Table 1, column 1.

References

Anderson DG, Levenberg S, Langer R. 2004. Nanoliter-scale synthesis of arrayed biomaterials and application to human embryonic stem cells. Nat Biotechnol 22:863–866.

Anderson DG, Putnam D, Lavik EB, Mahmood TA, Langer R. 2005. Biomaterial microarrays: Rapid, microscale screening of polymer–cell interaction. Biomaterials 26:4892–4897.

Bailey SN, Sabatini DM, Stockwell BR. 2004. Microarrays of small molecules embedded in biodegradable polymers for use in mammalian cell-based screens. Proc Natl Acad Sci USA 101:16144–16149.

Castel D, Pitaval A, Debily M-A, Gidrol X. 2006. Cell micrroarrays in drug discovery. Drug Discov Today 11(13/14):616–622.

Chambers I, Colby D, Robertson M, Nichols J, Lee S, Tweedie S, Smith A. 2003. Functional expression cloning of Nanog, a pluripotency sustaining factor in embryonic stem cells. Cell 113:643–655.

Davey RE, Zandstra PW. 2006. Spatial organization of embryonic stem cell responsiveness to autocrine Gp130 ligands reveals an autoregulatory stem cell niche. Stem Cells 24:2538–2548.

Dellatore S, Garcia A, Miller W. 2008. Mimicking stem cell niches to increase stem cell expansion. Curr Opin Biotechnol 19:534–540.

Dike LE, Chen CS, Mrksich M, Tien J, Whitesides GM, Ingber DE. 1999. Geometric control of switching between growth, apoptosis, and differentiation during angiogenesis using micropatterned substrates. In Vitro Cell Dev Biol Anim 35:441–448.

Diogo MM, Henrique D, Cabral JMS. 2008. Optimization and neural commitment of mouse embryonic stem cells. Biotechnol Appl Biochem 49:105–112.

Engler AJ, Sen S, Sweeney HL, Discher DE. 2006. Matrix elasticity directs stem cell lineage specification. Cell 126:677–689.

Even-Ram S, Artym V, Yamada KM. 2006. Matrix control of stem cell fate. Cell 126:645–647.

Fernandes AM, Fernandes TG, Diogo MM, da Silva CL, Henrique D, Cabral JMS. 2007. Mouse embryonic stem cell expansion in a microcarrier-based stirred culture system. J Biotechnol 132:227–236.

Fernandes TG, Kwon SJ, Lee M-Y, Clark DS, Cabral JMS, Dordick JS. 2008. On-chip, cell-based microarray immunofluorescence assay for high-throughput analysis of target proteins. Anal Chem 80:6633–6639.

Fernandes TG, Diogo MM, Clark DS, Dordick JS, Cabral JMS. 2009. High-throughput cellular microarray platforms: Applications in drug discovery, toxicology and stem cell research. Trends Biotechnol 27:342–349.

Fernandes TG, Fernandes-Platzgummer AM, da Silva CL, Diogo MM, Cabral JMS. 2010. Kinetic and metabolic analysis of mouse embryonic stem cell expansion under serum-free conditions. Biotechnol Lett 32:171–179.

Flaim CJ, Chien S, Bhatia SN. 2005. An extracellular matrix microarray for probing cellular differentiation. Nat Methods 2(2):119–125.

Flaim CJ, Teng D, Chien S, Bhatia SN. 2008. Combinatorial signaling microenvironments for studying stem cell fate. Stem Cells Dev 17:29–39.

Ha J, Engler CR, Lee SJ. 2008. Determination of diffusion coefficients and diffusion characteristics for chlorferon and diethylthiophosphate in Ca-alginate gel beads. Biotechnol Bioeng 100:698–706.

Horning JL, Sahoo SK, Vijayaraghavalu S, Dimitrijevic S, Vasir JK, Jain TK, Panda AK, Labhasetwar V. 2008. 3-D tumor model for in vitro evaluation of anticancer drugs. Mol Pharm 5:849–862.

Hubbel JA. 2004. Biomaterials science and high-throughput screening. Nat Biotechnol 22:828–829.

Khademhosseini A, Langer R, Borenstein J, Vacanti J. 2006. Microscale technologies for tissue engineering and biology. Proc Natl Acad Sci USA 108(8):2480–2487.

Kim M, Habiba A, Doherty J, Mills J, Mercer R, Huettner J. 2009. Regulation of mouse embryonic stem cell neural differentiation by retinoic acid. Dev Biol 328:456–471.

Klimanskaya I, Rosenthal N, Lanza R. 2008. Derive and conquer: Sourcing and differentiating stem cells for therapeutic applications. Nat Rev Drug Discov 7:131–142.

Ko IK, Kato K, Iwata H. 2005. Parallel analysis of multiple surface markers expressed on rat neural stem cells using antibody microarrays. Biomaterials 26:4882–4891.

Kwon SJ, Lee M-Y, Ku B, Sherman DH, Dordick JS. 2007. High-throughput, microarray-based synthesis of natural product analogues via in vitro methabolic pathway construction. ACS Chem Biol 2:419–425.

Lee M-Y, Park CB, Dordick JS, Clark DS. 2005. Metabolizing enzyme toxicology assay chip (MetaChip) for high-throughput microscale toxicity analyses. Proc Natl Acad Sci USA 102(4):983–987.

Lee M-Y, Kumar RA, Sukumaran SM, Hogg MG, Clark DS, Dordick JS. 2008. Three-dimensional cellular microarrays for high-throughput toxicology assays. Proc Natl Acad Sci USA 105(1):59–63.

McNeish J. 2004. Embryonic stem cells in drug discovery. Nat Rev Drug Discov 3:70–80.

Morrison S, Spradling A. 2008. Stem cells and niches: Mechanisms that promote stem cell maintenance throughout life. Cell 132:598–611.

Niwa H, Miyazaki J-I, Smith AG. 2000. Quantitative expression of Oct-3/4 defines differentiation, dedifferentiation or self-renewal of ES cells. Nat Genet 24:372–376.

Oyaas J, Storrø I, Svendsen H, Levine DW. 1995. The effective diffusion coefficient and the distribution constant for small molecules in calcium-alginate gel beads. Biotechnol Bioeng 47:492–500.

Siti-Ismail N, Bishop AE, Polak JM, Mantalaris A. 2008. The benefit of human embryonic stem cell encapsulation for prolonged feeder-free maintenance. Biomaterials 29:3946–3952.

Smith AG. 2001. Embryo-derived stem cells of mice and men. Annu Rev Cell Dev Biol 17:435–462.

Soen Y, Mori A, Palmer TD, Brown PO. 2006. Exploring the regulation of human neural precursor cell differentiation using arrays of signaling microenvironments. Mol Syst Biol 2:37.

Xu Y, Shi Y, Ding S. 2008. A chemical approach to stem-cell biology and regenerative medicine. Nature 453:338–344.

Ying Q-L, Nichols J, Chambers I, Smith A. 2003a. BMP induction of Id proteins suppresses differentiation and sustains embryonic stem cell self-renewal in collaboration with STAT3. Cell 115:281–292.

Ying Q-L, Stavridis M, Griffiths D, Li M, Smith A. 2003b. Conversion of embryonic stem cells into neuroectodermal precursors in adherent monoculture. Nat Biotechnol 21(2):183–186.

Ying Q-L, Wray J, Nichols J, Batlle-Morera L, Doble B, Woodgett J, Cohen P, Smith A. 2008. The ground state of embryonic stem cell self-renewal. Nature 453:519–523.